Artificial muscle based on coiled CNT yarns and biofriendly ionogels

Bin Ni, Loris Gelas, Gabriela Ananieva, Cédric Vancaeyzeele, Giao T M Nguyen, Frédéric Vidal, Cédric Plesse

Sensors & Actuators: B. Chemical 403 (2024) 135227

Contents lists available at ScienceDirect

Sensors and Actuators: B. Chemical

journal homepage: www.elsevier.com/locate/snb

Artificial muscle based on coiled CNT yarns and biofriendly ionogels

Bin Ni, Loris Gelas, Gabriela Ananieva, Cédric Vancaeyzeele [1], Giao T.M. Nguyen, Frédéric Vidal, Cédric Plesse *

CY Cergy Paris Université, Laboratoire de Physicochimie des Polymères et des Interfaces (LPPI), 95000 Neuville sur Oise, France

ARTICLE INFO

Keywords:
Carbon nanotube
Actuator
Ionogel
Ionic liquid electrolyte

ABSTRACT

A contractile ionic electrochemical actuator was designed by incorporating two coiled carbon nanotube (CNT) yarns coated with a biofriendly ionogel. The working principle of such an actuator stands in capacitive ionic accumulation at the electrochemical double layer, which converts into linear contraction of the coiled CNT yarns. The prepared ionogel showed a good ionic conductivity of up to 1.9 mS cm^{-1} at room temperature and suitable mechanical properties (Young modulus <1 MPa and elongation at break at 75%). The ionogel/coiled CNT yarn actuator exhibited a maximum contractile stroke of 1.78% under electrochemical stimulation in open air. Such yarn actuators with safe components could open opportunities for application prospects in smart textiles and biomedical devices.

1. Introduction

Contractile actuators based on yarns are promising and elegant precursors of artificial muscles for applications in smart textiles, prosthetics, soft robotics or exoskeletons [1,2]. Various types of yarn muscles have been reported since last decade, including conductive polymer yarns [3–5], shape memory alloy wires [6,7], twisted and coiled polyamide yarns [8,9], and carbon nanotube (CNT) yarns [10,11]. Among them, CNT yarn muscles are especially in the spotlight because of their high strength, high electrical conductivity over their entire length, and high energy conversion efficiencies, which have been driven either by humidity/solvent adsorption [12,13], thermal [14,15], or electrochemical [2,16,17] stimulation. In particular, electrochemically driven CNT muscles attracted significant interest from researchers due to their easy and desired electrical control as well as their low working voltages [13,18]. Their working principle relies on the charging/discharging of the electrochemical double layer (EDL) at the CNT-electrolyte interface through a capacitive process, transducing low-voltage electrochemical stimulation into a mechanical response. When the pristine CNT yarns are coiled by overtwisting, they can convert torsional actuation into a large tensile stroke [2].

Electrochemically driven CNT artificial devices induce *de facto* a need for ionic sources, such as organic ionic liquids [19–21], aqueous or organic electrolytes [22,23]. Lee et al. developed coiled CNT muscles with a contractile stroke up to 16.5% when immersed in organic electrolytes (0.2 M tetrabutylammonium hexafluorophosphate, TBA·PF_6, in propylene carbonate, PC) [17]. Qiao et al. designed a muscle composed of coiled CNT and graphene oxide (GO), which exhibited 8.1% stroke when immersed in aqueous electrolytes (0.5 M Na_2SO_4) [11]. Providing open-air actuation ability to these contractile actuators allows for a significant widening of their possible applications. It can be enabled by combining two coiled CNT yarns, respectively acting as anode and cathode, with a polymer gel containing electrolytes [2,21]. However, the design of the ionic source is of primary importance for integrating these artificial muscles into practical applications. Organic electrolytes endow the actuator with greater performance due to their larger electrochemical window and comparatively larger solvated ions [11]. Nevertheless, the toxicity of most organic solvents limits the application range of these actuators, especially in the fields of smart textiles, exoskeletons, and biomedical devices where contact with the human skin occurs. However, aqueous electrolytes suffer from a narrow electrochemical window and relatively small ion sizes, limiting the actuator stroke. Moreover, water or organic solvent evaporation, in open-air applications, will undoubtedly cause the loss of functional and actuation capability due to a significant drop of the ionic mobility [2]. .

Hence, electrolytes with high and air-stable ionic conductivity, such as ionogels, would allow the excellent implementation of CNT muscles. Ionogels are polymer gels containing solid polymer and ionic liquid (IL)

* Corresponding author.
E-mail addresses: gabriela.ananieva@cyu.fr (G. Ananieva), cedric.vancaeyzeele@cyu.fr (C. Vancaeyzeele), tran-minh-giao.nguyen@cyu.fr (G.T.M. Nguyen), frederic.vidal@cyu.fr (F. Vidal), cedric.plesse@cyu.fr (C. Plesse).
[1] ORCID: 0000–0002-9748–1562

https://doi.org/10.1016/j.snb.2023.135227
Received 8 September 2023; Received in revised form 18 December 2023; Accepted 22 December 2023
Available online 23 December 2023

phases that percolate throughout each other [24–26]. They are usually obtained by in situ polymerization of the gel network in the presence of ILs or by swelling a polymer network with ILs. Ionogels combine the mechanical properties of crosslinked polymer networks with the ionic conductivity, non-volatility, and non-flammability of ILs. To expand the potential applications of ionogels, it would be advantageous to promote the development of biofriendly materials. The toxicity of ionic liquids (IL) is dependent on the nature of their anion and their cation [27,28].

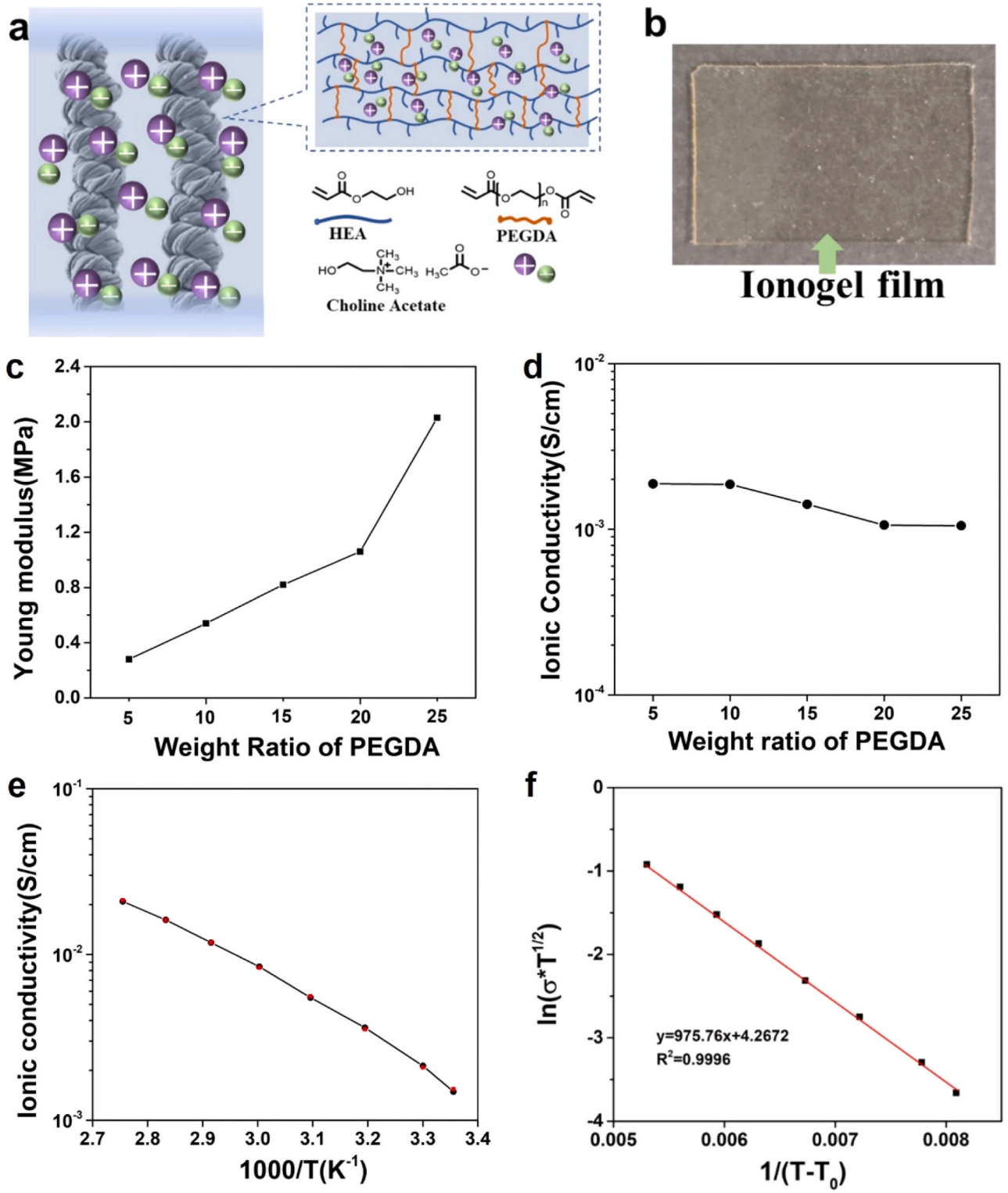

Fig. 1. (a) Schematic illustration of the electrochemical actuator and compound structure of biofriendly ionogels. (b) Image of an ionogel film with 5 wt% PEGDA crosslinker. (c) Young's modulus of ionogels with various crosslinker contents. (d) The ionic conductivity of ionogels with different crosslinker contents at room temperature. (e) The ionic conductivity of ionogels with 5 wt% crosslinker as a function of temperature. The red dot in the figure represents the experiment data and the blackline represents the calculation data from the VTF simulation. (f) Curves simulated by the VTF mode, using $T_0 = T_g$-50 K, resulting in A value of 71.31 S $K^{1/2}$ cm^{-1} and E_a of 8.11 kJ mol^{-1}.

Biobased ionic liquids (IL), appears as good candidates combining the non-volatile nature of ionic liquids with a lower toxicity [29]. They have already been considered as plasticizers of some polymers[30] or as biomolecule stabilizers in pharmaceutics, etc. [31,32]. However, most of these bio-sourced and biofriendly ILs have relatively high viscosity, resulting in low ionic conductivity, which reduces their interest in applications in electrochemical devices. However, choline based ionic liquids, and particularly choline acetate (ChAc), are very promising due to their relatively high ionic conductivity, reaching 3.9×10^{-3} S cm^{-1} for ChAc [27]. ChAc is composed of a choline cation from the vitamin B complex and an acetate anion from intracellular metabolites, which makes it belong to the category of biofriendly IL (Fig. 1a) [33,34]. Taking advantage of these properties, Elhi et al. demonstrated their interest in developing electrochemical actuators by the elaboration of bending tri-layer actuators based on polypyrrole electrodes and polyvinylidene fluoride (PVdF) / ChAc ionogel as the electrolyte, with an actuation strain of up to 0.67% [27]. The cytotoxicity experiments of choline acetate also showed a relatively low toxicity against HeLa cells compared to other choline ILs, such as choline malonate and choline isovalerate [27], demonstrating the good biofriendly properties of ChAc.

In this study, we investigated the synthesis of ChAc-based ionogels and their application as ionic coatings on coiled CNT yarns for the development of stable and biofriendly air-operating artificial muscles. The biofriendly ionogel coatings were synthesized by the free radical copolymerization of 2-hydroxyethyl acrylate (HEA) monomers and poly (ethylene glycol) diacrylate (PEGDA) crosslinkers [35,36] initiated by UV irradiation in the presence of ChAc. Gel formation was monitored by in-situ rheological measurements, and the resulting ionogels were characterized in terms of their ionic conductivity and mechanical properties. A coiled CNT yarn actuator was prepared by directly synthetizing the ionogel on the coiled CNT yarns. The ionogel acts an ionic source as well as a structuration glue for the constitution of the two-electrode CNT yarn actuator. The electrochemical properties and actuation performance of the resulting CNT-based actuators were characterized.

2. Material and methods

2.1. Materials

Choline Bicarbonate (80% in H_2O), poly(ethylene glycol) diacrylate (PEGDA, average Mn = 700 g mol^{-1}, 95.0%), 2-hydroxyethyl Methacrylate (HEMA, > 95.0%), Poly(ethylene glycol) dimethacrylate (PEGDMA, average Mn = 750 g mol^{-1}, 95.0%),and 2-hydroxy-2-methylpropiophenone 97% (darocur 1173) were purchased from Sigma-Adrich. Acetic acid (99.8%), was purchased from Honeywell. 2-hydroxyethyl Acrylate (HEA, > 95.0%) and choline chloride (ChCl, 98.0%) were purchased from TCI. Galvorn CNT yarns (diameter = 150 μm; resistance = 10 Ω m^{-1}) were purchased from DexMat,.

2.2. Synthesis of ionogels and fabrication of coiled CNT actuators

2.2.1. Synthesis of choline acetate

Choline acetate (ChAc) was synthesized via ion exchange. In brief, an acetic acid solution (50%wt) in water (10% excess) was added dropwise to a round-bottom flask filled with 50%wt choline bicarbonate in water. The mixture was then stirred at room temperature for 12 h. The remaining contaminants were removed by two successive extractions using ethyl acetate. Ethanol was then added to the aqueous solution to create a eutectic mixture. This solution was dried in rotavapor for 3 h under high vacuum for 12 h. The obtained white solid liquefies once it is hydrated. Yield 98%. Choline acetate: -N-CH_3: 3.05 ppm, N-CH_2: 3.89 ppm, CH_2-OH: 3.36 ppm, CH_3-CO-: 1.77 ppm.

2.2.2. Synthesis of acrylate-based ionogels

Appropriate amounts of PEGDA crosslinker were added to the HEA according to the formulation in Table 1, followed by the addition of choline acetate (50 wt% to the PEO precursor). Then, a solution of Darocure (0.1 g mL^{-1} in ethanol) was added to the mixture to reach 1 wt % of Darocure compared to the mass of PEGDA and HEA. The precursor solution was kept in the dark and then poured onto a glass plate with a Teflon mold (500 μm thick) in open air. The sample was polymerized using 15 scans on each side under a UV conveyer (Primarc UV Technology, Minicure, Mercury vapor lamp) with an irradiation power of 100 W cm^{-2}. The obtained ionogel film was dried under a dynamic vacuum for 1days at 50 ℃.

2.2.3. Synthesis of methacrylate-based ionogels

The ionogel was obtained by photopolymerization of HEMA crosslinked with PEGDMA using Darocur 1173 as the UV-photoinitiator soluble in the reactive mixture. The reactive mixture contains 48 wt% of HEMA, 2 wt% of PEGDMA, 0.75 wt% of Darocur1173 and 50 wt% of ChAc.

2.2.4. Fabrication of coiled CNT actuator

CNT yarns were first treated with ozone for 60 s then coated with unreacted ionogel precursors. The yarns were then overtwisted clockwise under a constant 5 MPa preload until a completely coiled state was reached (approximatively 50 turns cm^{-1}). The resulting coiled CNT yarns were UV-irradiated to trigger polymerization, thereby forming an ionogel coating. Two coated coiled CNT yarns were assembled using an extra layer of ionogel precursors as photocurable and ionic conducting glue to ensure a stable ionic junction between the two electrodes. Photopolymerization of the assembly leads to the formation of an actuator with a spacing of ~1 mm between the two electrodes, as shown in Fig. 2a.

2.3. Characterization

2.3.1. NMR characterization

^{1}H NMR spectra were recorded on a Bruker AVANCE 400 MHz spectrometer at 297 K with deuterated water (D_2O) as the solvent.

2.3.2. Mechanical properties

Traction experiments were carried out on a Dynamic Mechanical Analyzer (TAinst, Q800) in tensile mode at 30 ℃ with a strain rate of 100%·min^{-1} to 500%. To obtain stress-strain curves, an initial strain of 0.05% and a preload force of 0.01 N were performed.

2.3.3. Characterization of polymerization speed

The photopolymerization speed was recorded using a rheometer. Rheological measurements were performed using an Anton Paar Physica MCR 301 rheometer equipped with a CTD 450 temperature control device and a plate-plate geometry (gap 250 μm, diameter 25 mm, plate: polymerization system made from a lower glass plate coupled with a UV Source Omnicure 142 mW cm^{-2}). A deformation of 1% was imposed at a frequency of 1 Hz. The storage modulus (G′) and loss modulus (G″) were

Table 1
Detailed data on the mechanical properties of ionogels with various crosslinker contents.

Sample	Ionogel			Mechanical properties	
	HEA (wt %)	PEGDA (wt%)	ChAc[1] (wt%)	Young modulus (MPa)	Elongation at break (%)
1	75	25	100	2.03	25
2	80	20	100	1.06	36
3	85	15	100	0.82	39
4	90	10	100	0.54	37
5	95	5	100	0.28	75

[1] The weight contents of ChAc are given versus the weight of the PHEA-PEGDA network

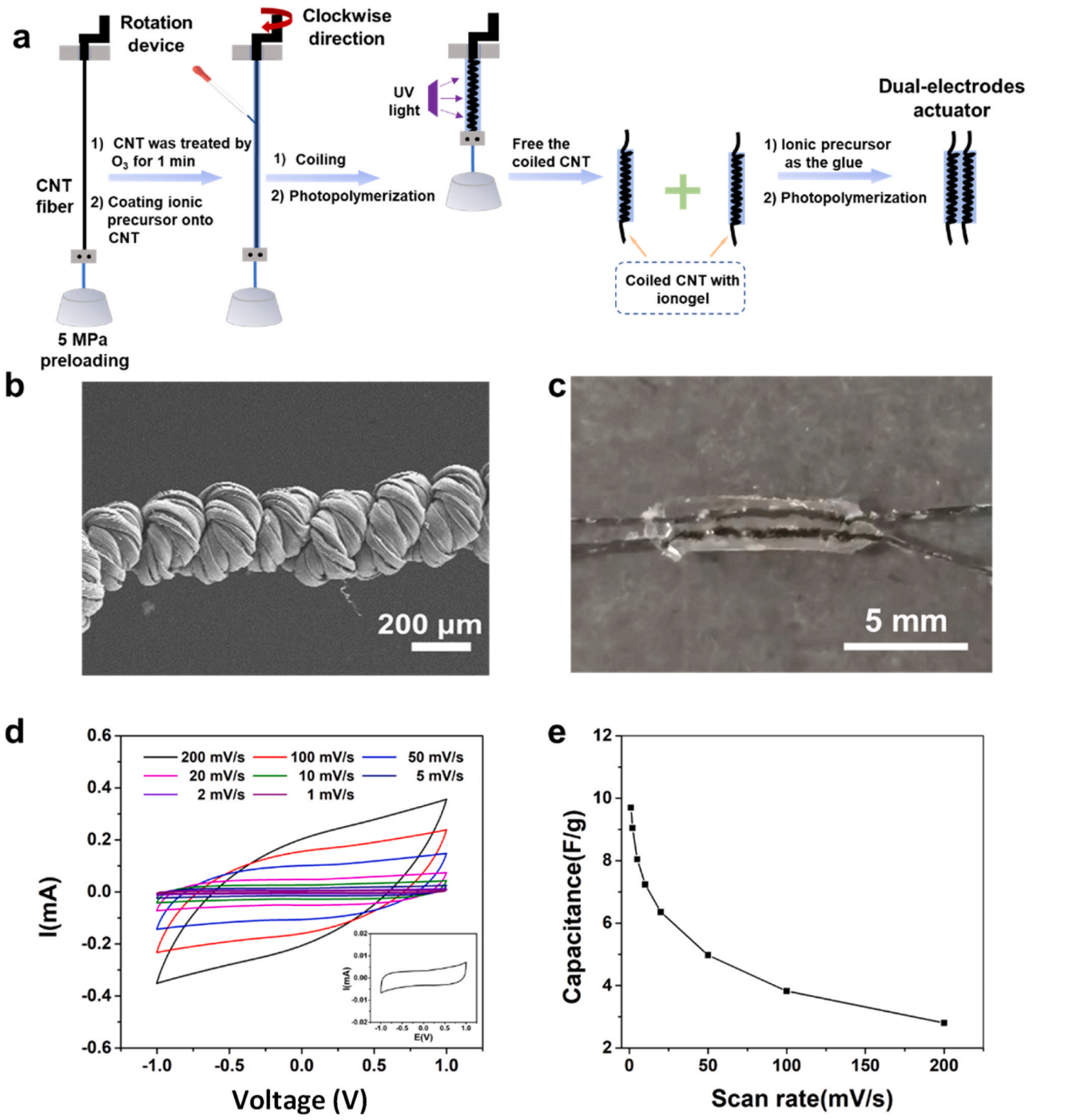

Fig. 2. (a) Schematic illustration of the coiling process of CNT and the preparation process of electrochemical actuators composed of two coiled CNT yarns coated by the PHEA/PEGDA 95/5 wt% + 100 wt% ChAc ionogel. (b) SEM image of coiled CNT yarn without ionic coating. (c) Photograph of the electrochemical actuator. (d) The CV scan curves of the electrochemical actuator at different scan rates. The inserted curve is a CV scan at 1 mV s^{-1}. (e) Capacitance of the electrochemical actuator at different scan rates.

recorded as functions of time. The solution of the precursor materials was placed in the rheometer geometry at 30 °C, measurements began immediately, and UV exposure was delayed in time.

2.3.4. Ionic conductivity

The ionic conductivity was recorded by electrochemical impedance spectroscopy using a VSP 150 potentiostat (Biologic SA). The samples were first dried under vacuum at 60 ℃ for 1 day before characterization. Experiments were carried out at different temperatures in a temperature-controlled oven in the frequency range from 2 MHz to 1 Hz at a rate of six points per decade and at 0 V with an oscillation potential of 10 mV. The ionic conductivity (S·cm^{-1}) is calculated using the equation.

$$\sigma = h/(Z^*S) \quad (1)$$

Where Z is the real part of the complex impedance (ohms), h is the thickness of the sample (cm), and S is the sample area (cm^2).

2.3.5. Scanning Electron Microscopy(SEM)

SEM was performed using a Carl Zeiss AG-ULTRA 55 by GEMINI with

a field emission gun at 2–10 kV.

2.3.6. Electrochemical characterization

2.3.6.1. Capacitance. The capacitance was calculated by cyclic voltammetry (CV) tests, which were performed by cycling the potential difference between + 1 V and –1 V for the dual-electrode actuator with biocompatible electrolytes at different scan rates using a two-electrode configuration at different scan rates. The capacitance was calculated by integration of Q to divide the range of potentials.

$$C=Q/V \quad (2)$$

2.3.7. Stroke deformation characterization

The length of the actuator was maintained by connecting it to an isometrically operated force-displacement lever arm transducer (Aurora Scientific model 300 C, Canada) with constant 25 mN preloading. The sensor recorded the stroke or force variation in real-time. The tensile stroke was calculated from the variation in actuator length ($\Delta l = l - l_0$) upon stimulation and the initial length of the actuator (l_0) using the following equation: strain $= \Delta l / l_0 \times 100$.

3. Results and discussion

3.1. Ionogel synthesis

ChAc was first synthesized according to a previously reported process,[27,37] as described in the Supporting Information (Scheme S1 and Fig. S1). The polymer network of the ionogel is a copolymer network of poly(2-hydroxyethyl acrylate) (PHEA) crosslinked with Polyethylene glycol diacrylate (PEGDA), which were chosen for their non-toxicity. [35,36] The network was prepared in the presence of 100 wt% ChAc ionic liquid with respect to the polymer network, i.e. 50 wt% of the final ionogel total weight, by free radical copolymerization of HEA monomer at different contents of PEGDA crosslinker (varying from 5 to 25 wt% compared to the monomer (HEA)). (Fig. 1a and Table 1). The reaction was initiated by 2-hydroxy-2-methylpropiophenone (HMP), a UV free-radical initiator. Similarly, an ionogel was prepared with methacrylate derivatives (Table S1 and Fig. S2 and S3).

The PHEMA/PEGDMA/ChAc ionogel resulted from the copolymerization of 2-hydroxyethyl methacrylate (HEMA) with polyethylene glycol dimethacrylate (PEGDMA) in the presence of 50 wt% ChAc, Ionogel formation kinetics were monitored by rheological analysis (Fig. S2). The ionogel precursor mixtures have a low viscosity of 0.74 Pa s and exhibit rapid gelation (<5 s and <8 s for acrylate and methacrylate based ionogels, respectively) once they are exposed to UV irradiation, which is an asset for a homogeneous and rapid polymerization of the ionic coatings onto CNT yarns [38]. The obtained ionogel films were transparent and slightly yellow, owing to the decomposition of the photoinitiator (Fig. 1b). Fig. 1c shows the mechanical properties of the ionogels as a function of crosslinker content. As expected, when the later decreases from 25 to 5 wt%, the ionogel's Young's modulus diminishes from 2.03 MPa to 0.28 MPa. In parallel, the elongation at break increased from 25% to a maximum of 75% with the decreasing crosslinker content. Thus, the mechanical properties of the ionogel could be tuned by adjusting the crosslinker content. Compared to acrylate-based material, the mechanical properties of methacrylate-based ionogel with 4% crosslinker revealed a more rigid and brittle material with a Young's modulus of 1.2 MPa and a strain at break of only 29% (Fig. S3). In the following section, only the results of the acrylate-based ionogel, i.e. PHEA/PEGDA/ChAc ionogel, will be reported.

Owing to the high ionic conductivity of neat ChAc (3.9×10^{-3} S cm^{-1})[27] and its high content of 50 wt% in the ionogel, as well as, its low glass transition temperature ($T_g = -48.6$ °C for the ionogel with 25 wt% crosslinker) (Fig. S4), the prepared PHEA/PEGDA/ChAc ionogel films displayed a high ionic conductivity, increasing slightly when decreasing the crosslinker content and reaching up to 1.9×10^{-3} S cm^{-1} for ionogel with 5 wt% crosslinker (Fig. 1d). The conduction behavior of the latter as a function of temperature was also investigated (Fig. 1e). The ionic conductivity increased to 10^{-2} S cm^{-1} at 80 °C. Moreover, the ionic conductivity measured as a function of the temperature is fitted by the empirical Vogel–Tammann–Fulcher (VTF) model[2] (Fig. 1f) [39], rather than classical and purely temperature dependent Arrhenius model[3] (Fig. 1e). This behavior indicates that ionic movements of the ChAc IL are thermally activated. However, their movements are correlated to those of the polymer chain segments of the host matrix expressed by their dependence on T_0, as observed for classical and non-biofriendly ionogels. A and Ea are parameters related to the number of charge carriers and the pseudo-activation energy for ion conduction, respectively. The parameter A was found to be 71.31 S $K^{1/2}$ cm^{-1} and Ea of 8.11 kJ mol^{-1}, which is close to the values reported for ionogels [26, 40–42]. Thanks to their combination of low initial viscosity, fast curing kinetics, high ionic conductivity, and good mechanical properties, this family of ionogels appears to be a promising photopolymerizable ionic coating for application as an ionic source in coiled CNT actuators.

3.2. Coiled CNT actuator fabrication

Coiled CNT yarns experiment considerably higher stroke strain than linear CNT yarns when submitted to electrical stimulation [10,17]. In this study, we used commercially available CNT yarns coiled by overtwisting in order to increase their electromechanical performance. The preparation process of the electrochemical actuator composed of coiled CNT yarns and ionogels coating is shown in Fig. 2a [43]. The ionogel composed of 5 wt% PEGDA was selected because it has the highest ionic conductivity, the highest elongation at break, and the lowest modulus. To ensure intimate contact at the interface between the electronically conducting CNT yarns and ionically conducting ionogel, the linear CNT yarns were first treated with ozone for 60 s to increase the wettability of the ionogel precursors to the CNT, and then coated with the unreacted ionogel precursors. Next, they were overtwisted clockwise under a constant 5 MPa preload until a completely coiled state was reached (approximatively 50 turns cm^{-1}). The coils appear with a relatively loose and open structure under these coiling conditions (Fig. 2b) when compared with the non-commercially available CNT yarns reported in the literature [2,17], but present the advantage of being obtained from a commercially available starting material. UV light was then used to initiate free-radical polymerization of the ionic coating precursors to obtain a homogeneous ionic coating on the surface of the coiled CNT yarn. Two coated coiled CNT yarns acting respectively as the anode and cathode were then assembled together with the photopolymerization of an extra layer of ionogel precursors, acting as photocurable and ionic conducting glue and ensuring stable ionic junction between the two electrodes. The obtained electrochemical actuator exhibited a spacing of ~1 mm between the two electrodes (Fig. 2c).

The electrochemical properties of the resulting device were examined using cyclic voltammetry in open-air in a two-electrode configuration from − 1 V to + 1 V at different scan rates (Fig. 2d). No noticeable Faradaic reactions were observed in this voltage range, and the charge capacity of the device decreased with increasing scan rate, as expected for this type of electrochemical system. The maximum capacitance was 9.7 F g^{-1} at a scan rate of 1 mV s^{-1} (Fig. 2e). In addition, when the voltage scan was from + 4 to − 4 V at a scan rate of 20 mV s^{-1}, similarly no significant Faradaic reaction was observed demonstrating the good electrochemical stability of the ionogel (Fig. S5).

[2] where E_a is activation energy, R: gas constant, T temperature in K and T_0 is reference temperature, typically T_g – 50 K

[3] where E_a is activation energy, R: gas constant and T temperature in K

3.3. Electromechanical performances

The electromechanical performance of the resulting actuators was then characterized in open-air under electrochemical stimulation (Scheme S2). The principle of operation relies on the electrochemical charging of the EDL, promoting the influx of ions into the electrodes. It promotes a local increase in volume and, consequently, an untwisting of the coil, expanding in diameter and contracting in length. Conversely, the efflux of ions during discharge promotes the opposite phenomenon and leads to the elongation of the coiled yarns. The deformation of such symmetric electrochemical devices is bipolar by nature, as shown in Fig. S6, and as previously reported for capacitive systems where both cations and anions are mobile [2]. A contraction was obtained during charging owing to ion influx by applying indifferently a positive or a negative potential difference. When switching from extremely positive to extremely negative voltages, the actuator presents a double motion, first elongating due to counter-ion efflux and then contracting due to the influx of oppositely charged ions.

Consequently, electromechanical characterizations were performed on only one side of the electrochemical window between 0 V (discharged EDL) and + 4 V (charged EDL). The EDL charging /uncharging processes of the electrodes are shown in Fig. 3a.

The slow accumulation of ions at the EDL layer, i.e. ion exflux and influx, along with a volume change of the yarn hindered by the loose and relatively open surface of the CNT, slows down the actuation. Therefore, advanced cyclic voltammetry (CVA) at 20 mV s^{-1} scan in a two-electrode configuration (Fig. 3b and c) was performed, in which the voltage was held at + 4 V and at 0 V for another 4 min in order to reach the maximum vertex voltage, to guarantee that complete ion influx and efflux occurred before the inverse sweep. As shown in Fig. 3c, the contractile stroke increased from 0.5% to 1.1% when the voltage was held at + 4 V for 4 min and then expanded to the original state for a 4 min holding at 0 V.

The electrochemical actuator was also actuated using different consecutive square potential waves with different pulse times. Fig. 4a depicts the actuator's stroke variation with a voltage plateau ranging from + 4 V to 0 V in a 60 s pulse time and demonstrates a reversible contraction/expansion of ~ 0.3%. Drift was observed in the electromechanical response owing to the mechanical relaxation of the coiled actuator under a preloaded force.

Subsequently, the dependence of the applied voltage and pulse time on the stroke variation was investigated. The stroke variation at

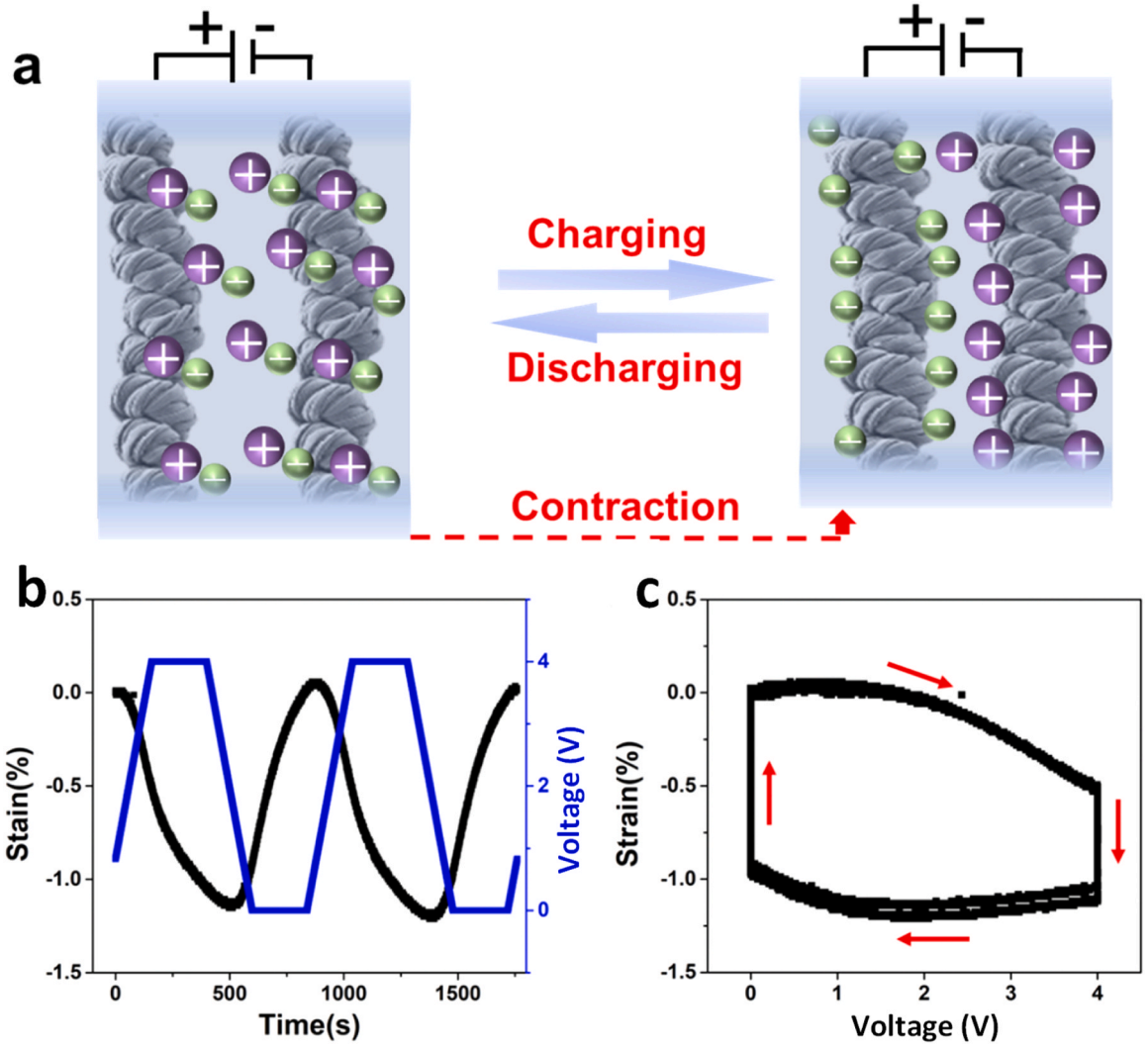

Fig. 3. (a) Mechanism of the electrochemical tensile stroke of an electrochemical actuator upon electrochemical stimulation. The actuator exhibited contraction when the ions swelled into the CNT yarns and recovered to the original state when the ions efflux from the yarns. (b) Advanced cyclic voltammetry (CVA) cycles for electrochemical tensile stroke measurements of the electrochemical actuator with a 25 mN preloading force. The voltage was scanned between 0 V and + 4 V at a scan rate of 20 mV s^{-1}, and then held at + 4 V and 0 V for another 4 min to ensure that the stroke reached its maximum and returned to its original value. (c) Electromechanical tensile stroke variation as a function of voltage with the CVA scan process. The red arrow indicates the direction of the stroke variation.

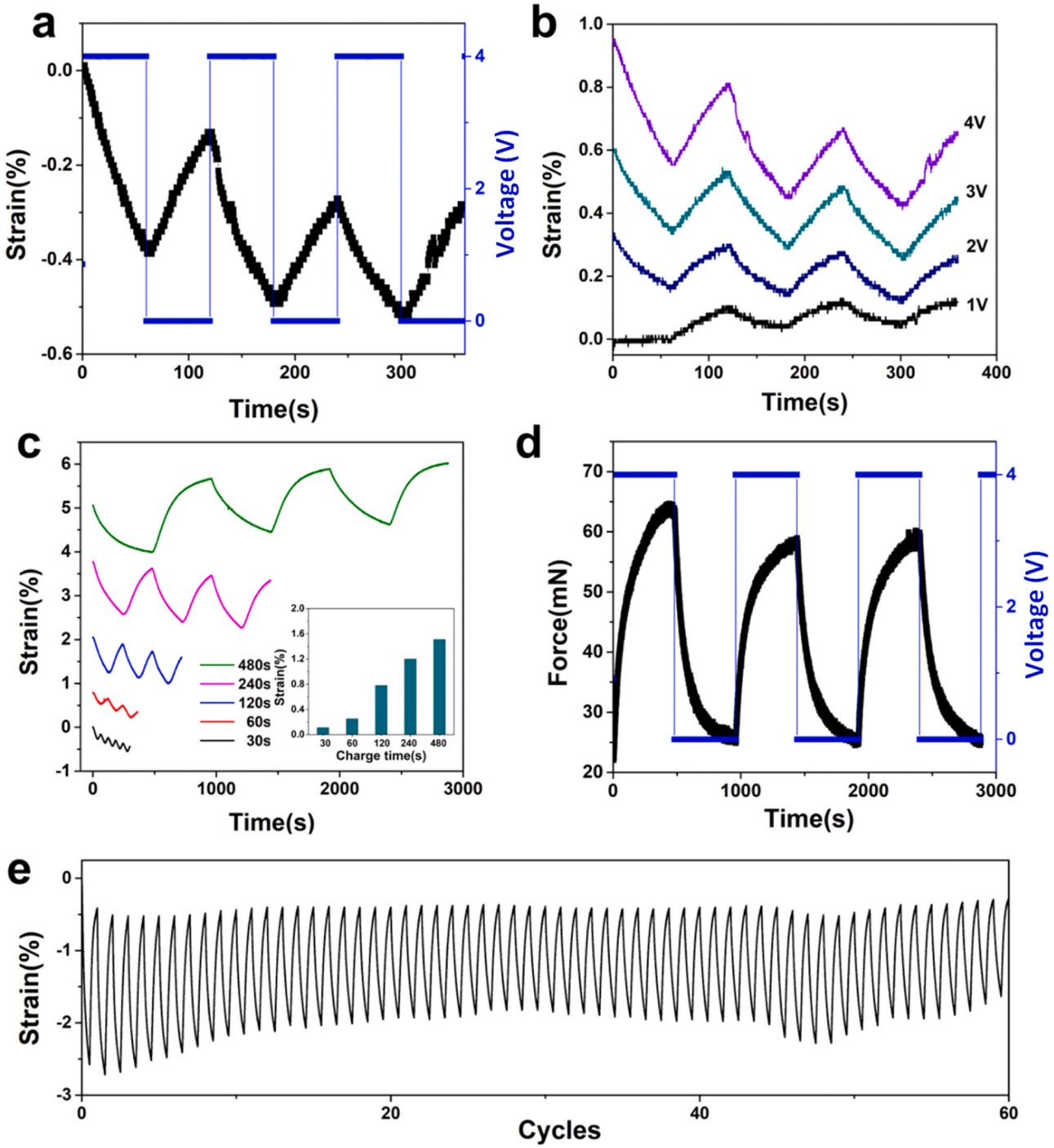

Fig. 4. (a) Chronoamperometry cycles for electrochemical tensile stroke measurements of an electrochemical actuator with a 25 mN preloading force. The square-wave potential changed from +4 to 0 V with a 60 s pulse time. (b) Stroke curves of the electrochemical actuator at different voltages changed from +1 V to +4 V vs 0 V square waves with a 60 s pulse time under a 25 mN preloading force. (c) Stroke variation of the electrochemical actuator as a function of pulse time with a 25 mN preloading force. The insert shows the maximum stroke values for different pulse times. The stroke was 1.7% with 480 s pulse time. (d) Generated force of stroke process for electrochemical actuator with a 1.25 N blocking force. (e) Stroke stability upon cycling of the electrochemical actuator in open air when applying a square wave potential changed from +4 to 0 V with a 480 s pulse under a 25 mN preloading force. There was no evident drop in stroke.

different voltage values was monitored during the same 60 s pulse time (Fig. 4b). The stroke increased with an increase in voltage, changing from 0.08% to ~ 0.3% when the voltage varied from +1 V to + 4 V. Different pulse times were also explored at a square-wave potential between 0 to +4 V (Fig. 4c). For a pulse time of 480 s, the maximum deformation reached 0.15 mm over an initial actuator length of 8.9 mm, corresponding to a stroke of 1.7%, because the stimulation duration was sufficiently long to fully charge the device.

Although the actuator strain is an important parameter for discriminating an actuator, the output force must be considered for practical applications. The blocking force of the actuator was then investigated under square-wave potential between +4 V to 0 V with a 480 s pulse time in isometric mode (initial blocking force of 1.25 N). As shown in Fig. 4d, the actuator was capable of generating a 35 mN force throughout the stroke process with a work capacity equal to 3.37 mJ g^{-1}. This work capacity is in the same order of magnitude as

that of the natural muscle (0.4–40 mJ g^{-1}) [44]. As a result, the actuator exhibits potential applications in artificial muscles. Finally, the stability of the actuator during cycling in open-air was investigated. As shown in Fig. 4e, after electrostimulation over 60 cycles with a square-wave potential between +4 V and 0 V with a 480 s pulse time, the strain remained almost constant at 1.5–1.7%, confirming the stability of these capacitive actuators for at least 16 h of continuous operation.

4. Conclusion

An electrochemical actuator was prepared by integrating coiled CNT composed of commercial linear CNT yarns coated with biofriendly ionogels composed of an acrylate polymer network with ChAc as the ionic source. The ionogel precursor mixtures possess a low viscosity (0.74 Pa.s at 30 ℃) and exhibited rapid gelation (<5 s under UV irradiation, which makes them suitable for yarn coating and upscalable to continuous coating of yarns. The ionogels exhibited high ionic conductivities of up to 1.9 $\times 10^{-3}$ S cm^{-1} and tunable mechanical properties (Young's modulus <1 MPa and elongation at break at 75%) by controlling the crosslinking density. The obtained actuator showed a controllable stroke, either by an applied voltage or pulse time. The maximum stroke attained was 1.7% upon electrochemical stimulation in open air, with an operating capacity of at least 16 h continuously. This biofriendly artificial muscle, with safe components for the environment, offers possibilities for applications in contact with the skin, such as electroactive textiles.

CRediT authorship contribution statement

Ni Bin: Writing – review & editing, Writing – original draft, Formal analysis. **Gelas Loris:** Investigation, Data curation. **Ananieva Gabriela:** Investigation, Formal analysis, Data curation. **Vancaeyzeele Cedric**: Writing – review & editing, Writing – original draft, Supervision, Investigation, Funding acquisition, Formal analysis, Data curation, Conceptualization. **Nguyen Giao T. M.:** Writing – review & editing, Writing – original draft, Validation, Supervision, Methodology, Funding acquisition, Formal analysis, Data curation, Conceptualization. **Vidal Frédéric:** Writing – review & editing, Writing – original draft, Validation, Supervision, Methodology, Funding acquisition, Formal analysis, Conceptualization. **Plesse Cédric:** Writing – review & editing, Writing – original draft, Validation, Supervision, Project administration, Methodology, Investigation, Funding acquisition, Formal analysis, Data curation, Conceptualization.

Declaration of Competing Interest

The authors declare the following financial interests/personal relationships which may be considered as potential competing interests: Bin Ni reports financial support was provided by European Union's Horizon 2020 research and innovation program under grant agreement no. 825232 WEAFING. Loris Gelas reports financial support was provided by European Union's Horizon 2020 research and innovation program under grant agreement no. 825232 WEAFING. Gabriela Ananieva reports financial support was provided by European Commission Marie Sklodowska-Curie Actions.

Data availability

Data will be made available on request.

Acknowledgments

B.Ni and L.Gelas would like to thank the European Union's Horizon 2020 Research and Innovation Program for financial support under grant agreement no. 825232 WEAFING. G. Ananieva would like to thank to European Union's Horizon Europe MSCA Doctoral Network SOFTWEAR, n°101072920. The authors would like to thank the Conseil regional île de France for funding the Cerasem project (grant: 15013107) that has allowed the acquisition of a ZEISS Gemini SEM 300.

Appendix A. Supporting information

Supplementary data associated with this article can be found in the online version at doi:10.1016/j.snb.2023.135227.

References

[1] A. Maziz, A. Concas, A. Khaldi, J. Stålhand, N.-K. Persson, E.W.H. Jager, Knitting and weaving artificial muscles, Sci. Adv. 3 (2017) 1–12, https://doi.org/10.1126/sciadv.1600327.
[2] H. Chu, X. Hu, Z. Wang, J. Mu, N. Li, X. Zhou, S. Fang, C.S. Haines, J.W. Park, S. Qin, N. Yuan, J. Xu, S. Tawfick, H. Kim, P. Conlin, M. Cho, K. Cho, J. Oh, S. Nielsen, K.A. Alberto, J.M. Razal, J. Foroughi, G.M. Spinks, S.J. Kim, J. Ding, J. Leng, R.H. Baughman, Unipolar stroke, electroosmotic pump carbon nanotube yarn muscles, Science 371 (80) (2021) 494–498, https://doi.org/10.1126/science.abc4538.
[3] J.D. Ryan, D.A. Mengistie, R. Gabrielsson, A. Lund, C. Müller, Machine-washable PEDOT:PSS dyed silk yarns for electronic textiles, ACS Appl. Mater. Interfaces 9 (2017) 9045–9050, https://doi.org/10.1021/acsami.7b00530.
[4] S. Aziz, J.G. Martinez, B. Salahuddin, N.K. Persson, E.W.H. Jager, Fast and high-strain electrochemically driven yarn actuators in twisted and coiled configurations, Adv. Funct. Mater. 31 (2021), https://doi.org/10.1002/adfm.202008959.
[5] R.H. Baughman, Conducting polymer artificial muscles, Synth. Met. 78 (1996) 339–353, https://doi.org/10.1016/0379-6779(96)80158-5.
[6] V.H. Ebron, Z. Yang, D.J. Seyer, M.E. Kozlov, J. Oh, H. Xie, J. Razal, L.J. Hall, J. P. Ferraris, A.G. MacDiarmid, R.H. Baughman, Fuel-powered artificial muscles, Science 311 (80) (2006) 1580–1583, https://doi.org/10.1126/science.1120182.
[7] Y. Song, S. Zhou, K. Jin, J. Qiao, D. Li, C. Xu, D. Hu, J. Di, M. Li, Z. Zhang, Q. Li, Hierarchical carbon nanotube composite yarn muscles, Nanoscale 10 (2018) 4077–4084, https://doi.org/10.1039/C7NR08595H.
[8] C.S. Haines, M.D. Lima, N. Li, G.M. Spinks, J. Foroughi, J.D.W. Madden, S.H. Kim, S. Fang, M. Jung de Andrade, F. Göktepe, Ö. Göktepe, S.M. Mirvakili, S. Naficy, X. Lepró, J. Oh, M.E. Kozlov, S.J. Kim, X. Xu, B.J. Swedlove, G.G. Wallace, R. H. Baughman, Artificial muscles from fishing line and sewing thread, Science 343 (80) (2014) 868–872, https://doi.org/10.1126/science.1246906.
[9] J. Chen, E. Pakdel, W. Xie, L. Sun, M. Xu, Q. Liu, D. Wang, High-performance natural melanin/poly(vinyl alcohol-co-ethylene) nanofibers/pa6 fiber for twisted and coiled fiber-based actuator, Adv. Fiber Mater. 2 (2020) 64–73, https://doi.org/10.1007/s42765-020-00036-w.
[10] R.H. Baughman, C. Cui, A.A. Zakhidov, Z. Iqbal, J.N. Barisci, G.M. Spinks, G. G. Wallace, A. Mazzoldi, D. De Rossi, A.G. Rinzler, O. Jaschinski, S. Roth, M. Kertesz, Carbon nanotube actuators, Science 284 (80) (1999) 1340–1344, https://doi.org/10.1126/science.284.5418.1340.
[11] J. Qiao, J. Di, S. Zhou, K. Jin, S. Zeng, N. Li, S. Fang, Y. Song, M. Li, R. H. Baughman, Q. Li, Large-stroke electrochemical carbon nanotube/graphene hybrid yarn muscles, Small 14 (2018), 1801883, https://doi.org/10.1002/smll.201801883.
[12] P. Chen, Y. Xu, S. He, X. Sun, S. Pan, J. Deng, D. Chen, H. Peng, Hierarchically arranged helical fibre actuators driven by solvents and vapours, Nat. Nanotechnol. 10 (2015) 1077–1083, https://doi.org/10.1038/nnano.2015.198.
[13] H. Cheng, Y. Hu, F. Zhao, Z. Dong, Y. Wang, N. Chen, Z. Zhang, L. Qu, Moisture-activated torsional graphene-fiber motor, Adv. Mater. 26 (2014) 2909–2913, https://doi.org/10.1002/adma.201305708.
[14] M.D. Lima, N. Li, M. Jung de Andrade, S. Fang, J. Oh, G.M. Spinks, M.E. Kozlov, C. S. Haines, D. Suh, J. Foroughi, S.J. Kim, Y. Chen, T. Ware, M.K. Shin, L. D. Machado, A.F. Fonseca, J.D.W. Madden, W.E. Voit, D.S. Galvão, R. H. Baughman, Electrically, chemically, and photonically powered torsional and tensile actuation of hybrid carbon nanotube yarn muscles, Science 338 (80) (2012) 928–932, https://doi.org/10.1126/science.1226762.
[15] S.M. Mirvakili, I.W. Hunter, Artificial muscles: mechanisms, applications, and challenges, Adv. Mater. 30 (2018), 1704407, https://doi.org/10.1002/adma.201704407.
[16] J.A. Lee, R.H. Baughman, S.J. Kim, High performance electrochemical and electrothermal artificial muscles from twist-spun carbon nanotube yarn, Nano Converg. 2 (2015), 8, https://doi.org/10.1186/s40580-014-0036-0.
[17] J.A. Lee, N. Li, C.S. Haines, K.J. Kim, X. Lepró, R. Ovalle-Robles, S.J. Kim, R. H. Baughman, Electrochemically powered, energy-conserving carbon nanotube artificial muscles, Adv. Mater. 29 (2017) 1–7, https://doi.org/10.1002/adma.201700870.
[18] G.V. Stoychev, L. Ionov, Actuating fibers: design and applications, ACS Appl. Mater. Interfaces 8 (2016) 24281–24294, https://doi.org/10.1021/acsami.6b07374.
[19] M. Ren, J. Qiao, Y. Wang, K. Wu, L. Dong, X. Shen, H. Zhang, W. Yang, Y. Wu, Z. Yong, W. Chen, Y. Zhang, J. Di, Q. Li, Strong and robust electrochemical artificial muscles by ionic-liquid-in-nanofiber-sheathed carbon nanotube yarns, Small 17 (2021), 2006181, https://doi.org/10.1002/smll.202006181.
[20] J. Foroughi, G.M. Spinks, G.G. Wallace, J. Oh, M.E. Kozlov, S. Fang, T. Mirfakhrai, J.D.W. Madden, M.K. Shin, S.J. Kim, R.H. Baughman, Torsional carbon nanotube

artificial muscles, Science 334 (80) (2011) 494–497, https://doi.org/10.1126/science.1211220.
[21] K.J. Kim, J.S. Hyeon, H. Kim, T.J. Mun, C.S. Haines, N. Li, R.H. Baughman, S. J. Kim, Enhancing the work capacity of electrochemical artificial muscles by coiling plies of twist-released carbon nanotube yarns, ACS Appl. Mater. Interfaces 11 (2019) 13533–13537, https://doi.org/10.1021/acsami.8b21417.
[22] K.M. Kim, J.A. Lee, H.J. Sim, K.-A. Kim, R. Jalili, G.M. Spinks, S.J. Kim, Shape-engineerable composite fibers and their supercapacitor application, Nanoscale 8 (2016) 1910–1914, https://doi.org/10.1039/C5NR07147J.
[23] Y. Yun, V. Shanov, Y. Tu, M.J. Schulz, S. Yarmolenko, S. Neralla, J. Sankar, S. Subramaniam, A multi-wall carbon nanotube tower electrochemical actuator, Nano Lett. 6 (2006) 689–693, https://doi.org/10.1021/nl052435w.
[24] Y. Zhong, G.T.M. Nguyen, C. Plesse, F. Vidal, E.W.H. Jager, Tailorable, 3D structured and micro-patternable ionogels for flexible and stretchable electrochemical devices, J. Mater. Chem. C. 7 (2019) 256–266, https://doi.org/10.1039/c8tc04368j.
[25] J. Le Bideau, L. Viau, A. Vioux, Ionogels, ionic liquid based hybrid materials, Chem. Soc. Rev. 40 (2011) 907–925, https://doi.org/10.1039/c0cs00059k.
[26] F. Li, G.T.M. Nguyen, C. Vancaeyzeele, F. Vidal, C. Plesse, Photopolymerizable ionogel with healable properties based on dioxaborolane vitrimer chemistry, Gels 8 (2022) 381, https://doi.org/10.3390/gels8060381.
[27] F. Elhi, H. Priks, P. Rinne, N. Kaldalu, E. Žusinaite, U. Johanson, A. Aabloo, T. Tamm, K. Põhako-Esko, Electromechanically active polymer actuators based on biofriendly choline ionic liquids, Smart Mater. Struct. 29 (2020), 055021, https://doi.org/10.1088/1361-665X/ab7f24.
[28] S.H. Zeisel, K.A. Da Costa, Choline: an essential nutrient for public health, Nutr. Rev. 67 (2009) 615–623, https://doi.org/10.1111/j.1753-4887.2009.00246.x.
[29] K. Radošević, M. Cvjetko Bubalo, V. Gaurina Srček, D. Grgas, T. Landeka Dragičević, I. Radojčić Redovniković, Evaluation of toxicity and biodegradability of choline chloride based deep eutectic solvents, Ecotoxicol. Environ. Saf. 112 (2015) 46–53, https://doi.org/10.1016/j.ecoenv.2014.09.034.
[30] G. Colomines, P. Decaen, D. Lourdin, E. Leroy, Biofriendly ionic liquids for starch plasticization: a screening approach, RSC Adv. 6 (2016) 90331–90337, https://doi.org/10.1039/C6RA16573G.
[31] E.E.L. Tanner, K.N. Ibsen, S. Mitragotri, Transdermal insulin delivery using choline-based ionic liquids (CAGE), J. Control. Release 286 (2018) 137–144, https://doi.org/10.1016/j.jconrel.2018.07.029.
[32] A. Banerjee, K. Ibsen, T. Brown, R. Chen, C. Agatemor, S. Mitragotri, Ionic liquids for oral insulin delivery, Proc. Natl. Acad. Sci. U. S. A. 115 (2018) 7296–7301, https://doi.org/10.1073/pnas.1722338115.
[33] A. Kaur, S. Bansal, D. Chauhan, K.K. Bhasin, G.R. Chaudhary, The study of molecular interactions of aqueous solutions of Choline Acetate at different temperatures, J. Mol. Liq. 286 (2019), 110878, https://doi.org/10.1016/j.molliq.2019.110878.
[34] J.M. Gomes, S.S. Silva, R.L. Reis, Exploring the use of choline acetate on the sustainable development of α-chitin-based sponges, ACS Sustain. Chem. Eng. 8 (2020) 13507–13516, https://doi.org/10.1021/acssuschemeng.0c05076.
[35] Z. Liu, S. Zhu, Y. Li, Y. Li, P. Shi, Z. Huang, X. Huang, Preparation of graphene/poly (2-hydroxyethyl acrylate) nanohybrid materials via an ambient temperature "grafting-from" strategy, Polym. Chem. 6 (2015) 311–321, https://doi.org/10.1039/C4PY00903G.
[36] J. Kim, T.E. Hefferan, M.J. Yaszemski, L. Lu, Potential of hydrogels based on poly (Ethylene Glycol) and sebacic acid as orthopedic tissue engineering scaffolds, Tissue Eng. Part A. 15 (2009) 2299–2307, https://doi.org/10.1089/ten.tea.2008.0326.
[37] N. Muhammad, M.I. Hossain, Z. Man, M. El-Harbawi, M.A. Bustam, Y.A. Noaman, N.B. Mohamed Alitheen, M.K. Ng, G. Hefter, C.-Y. Yin, Synthesis and physical properties of choline carboxylate ionic liquids, J. Chem. Eng. Data. 57 (2012) 2191–2196, https://doi.org/10.1021/je300086w.
[38] C. Huniade, D. Melling, C. Vancaeyzeele, G.T.M. Nguyen, F. Vidal, C. Plesse, E.W. H. Jager, T. Bashir, N.K. Persson, Ionofibers: ionically conductive textile fibers for conformal i-textiles, Adv. Mater. Technol. 7 (2022) 1–17, https://doi.org/10.1002/admt.202101692.
[39] S.B. Aziz, T.J. Woo, M.F.Z. Kadir, H.M. Ahmed, A conceptual review on polymer electrolytes and ion transport models, J. Sci. Adv. Mater. Devices 3 (2018) 1–17, https://doi.org/10.1016/j.jsamd.2018.01.002.
[40] G.T.M. Nguyen, A.L. Michan, A. Fannir, M. Viallon, C. Vancaeyzeele, C.A. Michal, F. Vidal, Self-standing single lithium ion conductor polymer network with pendant trifluoromethanesulfonylimide groups: Li+ diffusion coefficients from PFGSTE NMR, Eur. Polym. J. 49 (2013) 4108–4117, https://doi.org/10.1016/j.eurpolymj.2013.09.016.
[41] F. Li, G.T.M. Nguyen, C. Vancaeyzeele, F. Vidal, C. Plesse, Vitrimer ionogels towards sustainable solid-state electrolytes, RSC Adv. 13 (2023) 6656–6667, https://doi.org/10.1039/D2RA06829J.
[42] F. Li, G.T.M. Nguyen, C. Vancaeyzeele, F. Vidal, C. Plesse, Healable ionoelastomer designed from polymeric ionic liquid and vitrimer chemistry, ACS Appl. Polym. Mater. 5 (2023) 529–541, https://doi.org/10.1021/acsapm.2c01635.
[43] B. Ni, F.B. Ribeiro, C. Vancaeyzeele, G.T.M. Nguyen, E.W.H. Jager, F. Vidal, C. Plesse, Linear contracting and air-stable electrochemical artificial muscles based on commercially available CNT yarns and ionically selective ionogel coatings, Appl. Mater. Today 31 (2023), 101756, https://doi.org/10.1016/j.apmt.2023.101756.
[44] M. Duduta, E. Hajiesmaili, H. Zhao, R.J. Wood, D.R. Clarke, Realizing the potential of dielectric elastomer artificial muscles, Proc. Natl. Acad. Sci. U. S. A. 116 (2019) 2476–2481, https://doi.org/10.1073/pnas.1815053116.

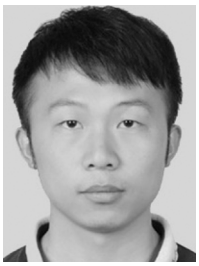

NI Bin obtained his Ph.D. in polymer chemistry from Chimie Paristech-Université PSL (France) in October 2020 , majored in thermal stimuli-responsive liquid crystal elastomers (LCEs). After completing his Ph.D. defense, he joined the LPPI in CY Cergy Paris Université (France) as a postdoctoral researcher. Now, he focuses on the fabrication of dry ionic gel for the electroactive yarns.

Gabriela Ananieva obtained her MsC in Textile Science from Saxion University of Applied Science (Netherland) in 2022 and started her PhD at CY Cergy Paris Université (France) in January 2023 in the frame of the Horizon Europe MSCA DN SOFTWEAR project. She is currently working on the develoepment of new electrocontracting yarn muscles for electroactive textiles by combining carbon nanotube yarns and ionoelastomers.

Cédric Vancaeyzeele obtained his PhD from University of Cergy-Pontoise in 2004. After one year as assistant professor, he gets a postdoc position at U of Toronto in M.A. Winnik group. Since his assignment in LPPI in 2006 as associate professor, his research focuses on the development of nanostructured polymer materials combining different properties for specific applications: polyisobutene based semi- IPN for sealing, amphiphilic materials synthesized by emulsion templating for fuel cell membrane or drug delivery, anion exchange IPN membranes for protection of air electrodes in metal-air batteries, protein base IPN as biomaterials or new bio-based thermoset…

Giao T. M. Nguyen received her PhD degree (2003) on Chemistry and Physico-chemistry of Polymer from University of Maine (France). She then joined Prof. Bo Nyström's group in Oslo University (Norway) as a postdoctoral fellow (2004–2005) working on the modification of polysaccharides. In 2008, she joined LPPI University of Cergy Pontoise (France) as assistant professor and then as postdoctoral fellow (2009–2010) on the synthesis of polyelectrolyte for using as Li-batteries solid electrolyte. She is associated professor since 2010. Her current interests focus on the development of new electrolyte polymer system for applications in electrochemical devices such as actuators, hybrid photovoltaic systems, Li-batteries.

Frédéric Vidal received his Ph.D. in polymer chemistry from Lyon University in 1995. He then joined Eindhoven Technology University as a postdoctoral fellow in 1995. He moved to University of Cergy-Pontoise (UCP) as an associate professor in 1997. Currently, he is full professor at UCP, a position he has held since 2008. From 2009 to 2018, he was appointed director of the laboratory of Physicochemisty of Polymers and Interfaces. His research includes development of Interpenetrating Polymer Networks (IPNs), conducting polymers and conducting IPNs based electrochemical devices such as electrochromic devices or actuators.

Cédric Plesse obtained his PhD (2004) in macromolecular chemistry at the University of Cergy-Pontoise (France). His research consisted in developing conducting semi-interpenetrated polymer networks to produce actuators. He received in 2005 the french PhD Prize by the Groupe Français des Polymères (GFP). He then joined Prof. Mario Leclerc's laboratory at the University of Laval (Canada) as a postdoctoral researcher (2004–2006) to synthesize conjugated polymers as transducers for DNA biochips. He was then recruited as Associate Professor at the Laboratory of Physicochemistry of Polymers and Interfaces (LPPI) at the University of Cergy-Pontoise in 2006, and obtained his habilitation (HDR) in 2014. He was promoted full professor at CY Cergy Paris University in 2021. His main research themes concern the development of smart and electroactive materials, including conducting polymers actuators, textile muscles, smart ionogels and self-healing materials.